

PHYSICAL REVIEW B

CONDENSED MATTER

THIRD SERIES, VOLUME 46, NUMBER 23

15 DECEMBER 1992-I

Electronic structure, lattice stability, and superconductivity of CrC

David J. Singh and Barry M. Klein*

Complex Systems Theory Branch, Naval Research Laboratory, Washington, D.C. 20375-5000

(Received 27 July 1992)

Electronic-structure and total-energy calculations are used to elucidate the properties of the recently synthesized NaCl-structure CrC phase. The lattice parameter, elastic constants, Γ -point optic-phonon frequency, and formation energy are determined using total-energy methods. No sign of lattice instabilities is found, indicating that NaCl-structure CrC is a true metastable phase. In fact, the elastic constants and optic-phonon frequency have values comparable to those in other known NaCl-structure transition-metal carbides. On the other hand, and in contrast to VC and NbC, CrC is found to be unstable with respect to phase separation into C and Cr, explaining the difficulty of its synthesis. The electronic structure is qualitatively similar to that of TiC and VC except for the placement of the Fermi level E_F . A relatively high density of states at E_F , which is derived from weakly hybridized Cr d states, is found. However, fixed-spin-moment calculations show that this does not lead to a ferromagnetic instability. Rigid muffin-tin approximation electron-phonon-interaction calculations lead to a prediction that CrC is a superconductor with a transition temperature in the range 5–10 K.

I. INTRODUCTION

The NaCl-structure transition-metal carbides are unusual in several respects. They are generally very hard, corrosion-resistant, high-melting-temperature metals. These desirable properties are understood to arise in large part from strong covalent transition-metal- d -carbon- p bonding.¹ Among the $3d$ materials, TiC has the highest melting temperature, suggesting the strongest bonding. VC, which has one more valence electron, forms with C vacancies and has a lower melting temperature. Until very recently,² there were no accepted reports of the synthesis of NaCl-structure CrC, which is the next member of the series.

Early self-consistent band-structure calculations³ for these materials have led to a description of the bonding of these materials, which has been supported by subsequent studies.^{4–6} In TiC, which, as mentioned, is expected to have the strongest bonding, the Fermi energy (E_F) lies in a pronounced pseudogap in the electronic density of states (DOS), leading to a low DOS at E_F , $N(E_F)$. The states below E_F are dominated by strongly hybridized bonding combinations of Ti $3d$ orbitals of e_g symmetry and C p -derived orbitals, with some contribution from Ti-Ti $t_{2g}\sigma$ and C p -Ti $t_{2g}\pi$ bonding orbitals. Both the Ti e_g -C p antibonding states and most of the Ti t_{2g} -derived states are found in the region above the pseudogap, although the latter provide by far the largest contribution to the DOS in this region.

The electronic structure of VC is related to that of TiC by rigid band behavior (a rather general feature of the transition-metal carbides); the two-band structures are qualitatively similar, differing primarily in the position of E_F . In VC, E_F lies one electron higher than in TiC, leading to some occupation of the antibonding and/or non-bonding states (see below) above the pseudogap, and thereby offering an explanation of the apparently weaker bonding in VC.

Zhukov and co-workers⁵ have reported a local-density approximation (LDA)-based electronic structure and some total-energy calculations for CrC which, as mentioned, is the next member of the series. They find once again that, at least qualitatively, the electronic structure is related to that of TiC by rigid band behavior, and that in CrC, E_F falls near a pronounced peak in the DOS, which is derived from weakly hybridized Cr d states. They remark that the additional electron in CrC leads to the occupation of additional antibonding states and that this explains the difficulty in synthesizing CrC. This is, however, somewhat at odds with their calculated bulk modulus, which is significantly higher than that of TiC. Based on this elevated bulk modulus and some other considerations, they predict that CrC has the greatest strength in the series. They did not, however, examine the lattice stability or other properties of CrC, which could be anomalous because of the high DOS at E_F .

Very recently, Liu and Cheng² have reported synthesis of NaCl-structure CrC by carbon-ion implantation into

Cr films. Further, they have determined that, although stable at room temperature, the CrC phase is unstable above 250 °C, possibly because of the presence of oxygen. These results suggest that NaCl-structure CrC is a true metastable phase, possibly with weaker bonding than TiC and VC. There are, however, other possibilities. For example, the observed NaCl phase could be stabilized by the presence of impurities or by an off-stoichiometric composition. The purpose of the present paper is to elucidate the properties of NaCl-structure CrC, using LDA-based electronic-structure and total-energy calculations.

We calculate the electronic structure, lattice parameter, and bulk modulus, as did Zuhkov *et al.*, but using the general potential linearized augmented plane-wave (LAPW) method,⁷ which is free from shape approximations. Further, we study the bonding and lattice stability by calculating the enthalpy of formation (ΔH_f), elastic constants, and Γ -point optic-phonon frequency, ν_{opt} (note that for the NaCl-structure metallic carbides, the transverse and longitudinal branches are degenerate at Γ).

It is often the case that an elevated $N(E_F)$ is associated with magnetic instabilities, frequently towards ferromagnetism. Accordingly, we have performed fixed spin-moment calculations,⁸ searching for a ferromagnetic state for CrC. Although we have not ruled it out, we do not expect itinerant antiferromagnetism, because even with a substantial superexchange interaction between neighboring Cr atoms, an antiferromagnetic ground state could be frustrated by the fcc lattice.

Superconductivity is quite common among the NaCl-structure transition-metal carbides and nitrides, and it is often the case that an elevated $N(E_F)$ is favorable for superconductivity provided, of course, that it does not result in magnetism or structural instabilities. We investigated the possibility of superconductivity in CrC by evaluating the McMillan-Hopfield parameter, $\eta = \langle I^2 \rangle N(E_F)$, where $\langle I^2 \rangle$ is an electron-ion matrix element, which we calculated in the rigid muffin-tin approximation (RMTA).⁹

II. METHOD

As mentioned, the calculations reported here were performed using the general potential LAPW method.⁷ This method imposes no shape approximations on either the potential or the charge density (except that deep core states are constrained to be spherical). A local orbital extension¹⁰ was used to relax the linearization and to include the Cr 3s and 3p core states with the valence states in a single energy window. The calculations were performed within the LDA using the Hedin-Lundqvist exchange-correlation function.¹¹ Both the core and valence states were treated self-consistently, the valence states in a scalar-relativistic approximation and the core states relativistically in a spherical approximation. A well-converged basis consisting of approximately 190 functions was used,¹² and self-consistency was obtained using a sampling of 60 special \mathbf{k} points¹³ in the irreducible $\frac{1}{48}$ of the Brillouin zone. The Fermi energy and electronic DOS were obtained from a Fourier interpolation¹⁴

of the self-consistent energy bands, which were calculated at 145 uniformly distributed points in the irreducible wedge.

The lattice parameter, elastic constants, ν_{opt} , and ΔH_f were obtained using total-energy calculations. ΔH_f was determined using well-converged parallel total-energy calculations for bcc Cr, diamond-structure C, and CrC, and was corrected using the very small experimental energy difference¹⁵ between diamond and graphite.

A cubic crystal has three independent elastic constants, which can be taken as the bulk modulus $B = (c_{11} + 2c_{12})/3$ and the two shear constants c_{44} and $(c_{11} - c_{12})$. These were determined as in Ref. 16; B was determined by fitting the calculated total energy as a function of the lattice parameter to an equation of state (in this case, the Murnaghan form¹⁷). The shear elastic constants were calculated from the total energy as a function of volume-conserving orthorhombic (for $c_{11} - c_{12}$) and monoclinic (for c_{44}) strains at the equilibrium lattice parameter. As mentioned, 60 special \mathbf{k} points were used for the equation of state. Meshes with the same densities were used for the strained lattices, but because of the reduced symmetry the actual number of independent \mathbf{k} points was larger, 306 and 256 for the monoclinic and orthorhombic strains, respectively. ν_{opt} was determined, using the frozen-phonon technique, by calculating the total energy as a function of a displacement of the C atom along a cube axis, and extracting the quadratic term. The same \mathbf{k} -point density was used as for the elastic-constant calculations. Parallel calculations (see below) were performed for VC and for NbC, to provide comparisons and to check our procedures.

The fixed spin-moment method⁸ was used to determine whether or not CrC has a ferromagnetic instability. For this purpose, the total energy was calculated as a function of the imposed spin moment at the calculated equilibrium lattice parameter. In these self-consistent calculations, a Brillouin-zone sampling of 182 special \mathbf{k} points in the irreducible wedge was used. Calculations were performed for moments between zero and 1.5 μ_B per formula unit.

In the RMTA, the muffin-tin components of the McMillan-Hopfield parameter are given by

$$\eta_\alpha = \frac{E_F}{\pi^2 N(E_F)} \sum_l 2(l+1) \sin^2(\delta_{l+1}^\alpha - \delta_l^\alpha) \frac{N_l^\alpha N_{l+1}^\alpha}{N_l^{(1)\alpha} N_{l+1}^{(1)\alpha}}, \quad (1)$$

where the δ_l^α are the scattering phase shifts at E_F for atom α and angular momentum l . $N_l^{(1)\alpha}$ are the single scatterer densities of states, as defined in Ref. 9, and N_l^α are site-dependent projected densities of states, again at E_F . These parameters are obtained from the calculated band structure and the self-consistent potential (the spherical component of the potential is used in RMTA calculations). The McMillan equation may then be used to estimate the superconducting transition temperature,

$$T_c = \frac{\langle \omega \rangle}{1.45} \exp \left[- \frac{1.04(1+\lambda)}{\lambda - \mu^* - 0.62\lambda\mu^*} \right], \quad (2)$$

with

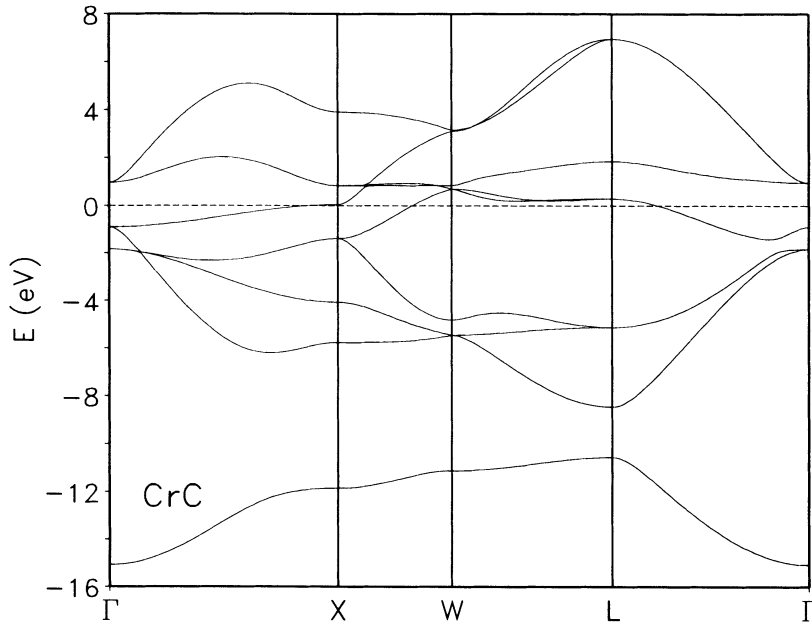


FIG. 1. Band structure of NaCl-structure CrC at the calculated equilibrium lattice parameter of 7.578 a.u. The dashed line denotes E_F .

$$\lambda = \sum_{\alpha} \left[\frac{\eta}{M \langle \omega^2 \rangle} \right] \alpha, \quad (3)$$

where the sum on α is over the different atoms in the unit cell and $\langle \omega^2 \rangle$ and $\langle \omega \rangle$ are averages of phonon frequencies. While we do not know the phonon spectrum of CrC, we can make estimates based on the elastic constants, ν_{opt} , and knowledge of the phonon frequencies in NbC, which we find to have similarities to CrC (see below).

III. RESULTS AND DISCUSSION

A. Electronic structure

The band structure of CrC at the LDA equilibrium lattice parameter of 7.578 a.u. is shown in Fig. 1 and the corresponding projected DOS is shown in Fig. 2. The projected DOS for VC at its equilibrium lattice parameter, which was obtained from parallel calculations, is shown in Fig. 3 for comparison purposes. As may be seen from Fig. 1, the C s -derived band lies approximately 12 eV below E_F and is separated from the valence bands by a minimum of 2 eV (at L). The valence bands, which extend from approximately 8 eV below E_F to 7 eV above it, consist of strongly hybridized Cr e_g -C p and more weakly hybridized Cr t_{2g} -derived bands. The flat bands near E_F are of the latter type. Our calculated DOS is similar in shape to that of Zhukov and co-workers⁵ but there are important quantitative differences. Most significantly, $N(E_F)$ in the present calculation is 27.9 states/Ry, which is approximately twice the value they obtained. Further, the details of the peak structures and the relative heights of the peaks in their DOS differ from the present results. We do not know the reason for these differences. Although we are not familiar with the details of their calculations, we note that it seems unlikely that

the combined effects of the slightly different lattice parameter and the shape approximations in their atomic-sphere-approximation calculations could fully account for them.

Comparing the projected DOS of Figs. 2 and 3, it is apparent that the differences between VC and CrC are well

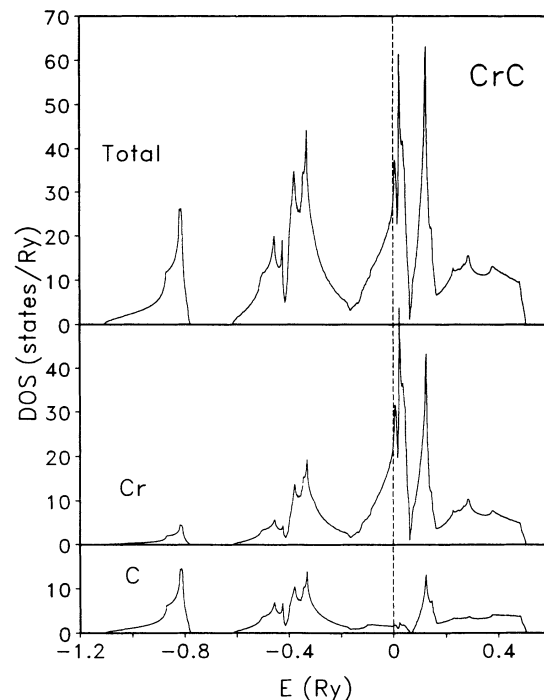


FIG. 2. Total and projected DOS of CrC at the calculated equilibrium lattice parameter. The projections are the DOS in states/Ry. f.u.) with each state weighted by its integrated charge inside the corresponding LAPW sphere. The radii of the spheres are 2.0 a.u. for Cr and 1.7 a.u. for C. The dashed vertical line denotes E_F .

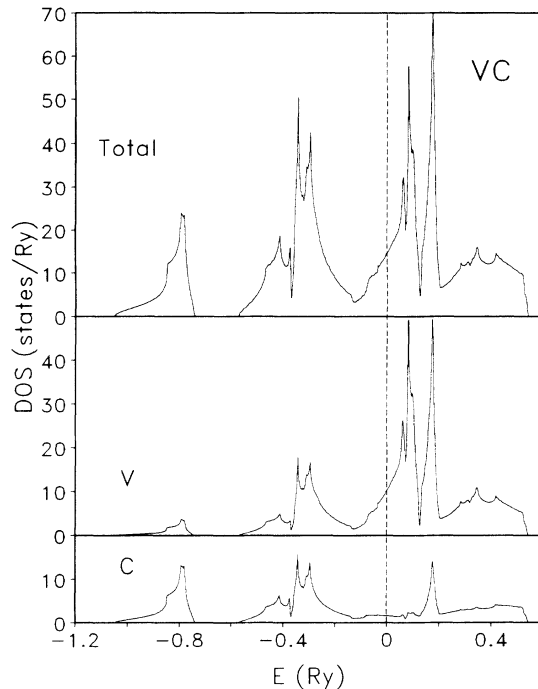


FIG. 3. Total and projected DOS of VC at its calculated equilibrium lattice parameter (see Fig. 2 caption).

described by rigid band behavior. The peak structure and character of the bands is preserved. The main difference, apart from the position on E_F , is the slightly narrower pseudogap in the valence bands of CrC. In both VC and CrC, E_F occurs on the low-energy side of a metal t_{2g} -derived peak in the DOS, although it is much closer to the peak in CrC. [$N(E_F) = 14.6 \text{ Ry}^{-1}$ for VC is approximately half that of CrC.] Accordingly, one might expect the differences between VC and CrC and, for that matter, along the series TiC-VC-CrC, to be dominated by the states comprising this peak. The projected DOS (Fig. 2) shows that the contribution to this peak from C-derived states is very small and, therefore, it cannot be described as being comprised of Cr d -C p antibonding states. These lie at higher energies, as evidenced by the greatly increased C participation in the DOS starting with the next peak (approximately 1.2 eV higher).

B. Energetics

The elastic constants, ν_{opt} , and ΔH_f provide information regarding the bonding and the effects of occupying the t_{2g} -derived states near E_F . Results for CrC are listed in Table I, along with values for VC and NbC obtained from parallel calculations, except for the elastic constants of NbC, which are from calculations by Chen *et al.*,¹⁸ who used a very similar method.

The calculated value of ΔH_f explains the difficulty in synthesizing CrC. In particular, the fact that ΔH_f is positive means that CrC is not a stable phase. This is in contrast to VC and NbC, both of which are predicted by parallel calculations to be stable phases, in agreement with experiment. The experimental ΔH_f for NbC from

TABLE I. Calculated properties of CrC, VC, and NbC. All calculations are at the calculated equilibrium lattice parameter a . ν_{opt} is the transverse optic-phonon frequency and ΔH_f is the heat of formation. The numbers in parentheses are experimental values.

| | CrC | VC | NbC |
|--------------------------|---------------------|-------|---------------------|
| a (Å) | 4.01 | 4.10 | 4.45 |
| a (Å) | (4.03) ^a | | (4.47) ^b |
| B (GPa) | 333 | 351 | 332 ^c |
| $c_{11} - c_{12}$ (GPa) | 581 | 570 | 460 ^c |
| c_{44} (GPa) | 140 | 203 | 140 ^c |
| ν_{opt} (THz) | 15.6 | 18.2 | 16.8 (16.6) |
| ΔH_f (eV/f.u.) | 0.16 | -1.06 | -1.22 |

^aReference 2.

^bC.P. Kempter, E. K. Storms, and R. J. Fries, *J. Chem. Phys.* **33**, 1873 (1960).

^cLAPW calculations of Ref. 18; experimental values from neutron scattering are quoted in Ref. 20.

thermochemical measurements¹⁹ is -1.43 eV/f.u. , which is 0.21 eV/f.u. different from the value we calculate. Although the errors are expected to be somewhat smaller for CrC (because the bonding of Nb is much stronger than that of Cr; 7.6 eV/atom versus 4.1 eV/atom)¹⁹ we interpret the difference between the calculated and experimental ΔH_f for NbC as an indication of the reliability of the calculated values for CrC and VC. Thus, we may conclude that CrC is unstable, with a small positive enthalpy of formation, thereby explaining the difficulty in synthesizing it by conventional means, but not contradicting its formation through highly nonequilibrium processes, as in the ion-implantation experiment of Ref. 2.

C. Lattice stability, elastic constants, and optic-phonon frequency

The optic phonon involves motion of the C sublattice relative to the transition-metal sublattice and thus is determined by the force constants that couple metal and C atoms. The dominant contributions²⁰ to these are from the nearest-neighbor interaction. A weakening of the metal-C covalent bonds in CrC relative to VC would be reflected in a reduction in ν_{opt} . (Note that the reduced mass entering the phonon frequency is dominated by the light C atom so that while mass differences should be considered in a quantitative analysis, they can be ignored in qualitative statements such as the preceding). Conversely, evidence that these bonds are not weakened in CrC would be provided if ν_{opt} for the two materials were essentially the same. An examination of Table I reveals that the ν_{opt} for CrC is reduced by 14% relative to VC (a change in the effective force constant of 27%), and is 7% lower than ν_{opt} for NbC. We note that the calculated $\nu_{\text{opt}} = 16.8 \text{ THz}$ of NbC is in very good agreement with the experimental value²¹ of 16.6 THz . These results imply some weakening of the metal-carbon bonds in CrC, although they remain quite strong.

Unlike ν_{opt} , the elastic constants contain information not only about the transition-metal-C bonding, but also

about the t_{2g} -mediated direct bonding between the transition-metal atoms. Weber,²⁰ by fitting phonon spectra to a sophisticated model, has shown that the force constants arising from these interactions, although less important than the metal-C interactions, are substantial in the transition-metal carbides. As may be noted from Table I, the calculated elastic constants for CrC are quite high, and the elastic-stability criteria are well satisfied. This, and the stable optic phonon, lead to the prediction that CrC is a true metastable phase, supporting the measurements of Ref. 2. Moreover, the calculated lattice parameter $a = 4.01 \text{ \AA}$ is in excellent agreement with that reported in Ref. 2 (4.03 \AA), lending additional support to the identification of the phase as NaCl-structure CrC.

We obtain a bulk modulus for CrC that is 5% smaller than that of VC. This is in contrast to the result of Zhukov *et al.*⁵ but is in agreement with the expectation of weaker bonding in CrC. We note that experimental elastic constants are available for near-stoichiometric NbC,^{20,21} and these are in very good agreement with the calculations of Chen *et al.*,¹⁸ which are very similar to those presented here. (Our value for the bulk modulus of NbC is 326 GPa, essentially identical to that of Ref. 18).

The shear moduli of CrC, like the bulk modulus, are generally lower than the corresponding moduli in VC. We find that c_{44} , which involves shearing the metal-C bonds, is approximately 30% lower in CrC than in VC; ($c_{11} - c_{12}$), which involves stretching (and compression) of metal-C bonds with a combination of bending and stretching of metal-metal bonds,²² is slightly higher in CrC. Taking the different lattice parameters of VC and CrC into account, this means that the effective force-constant determining c_{44} is approximately 34% lower in CrC than in VC, that determining B is 9% lower, and that determining ($c_{11} - c_{12}$) is only 2% lower.

The reduced value of c_{44} in CrC is consistent with the reduction in ν_{opt} . This supports our earlier conclusion that the metal-C bonds are somewhat weaker in CrC than in VC. We emphasize, however, that the states being occupied in going from VC to CrC are not the metal-C antibonding states, and occupation of antibonding states is not behind this weakening. Rather, occupation of the *bonding* states below the pseudogap in CrC yields an intrinsically weaker bond than occupation of the corresponding states in VC. The fact that B decreases more rapidly than ($c_{11} - c_{12}$) suggests a small strengthening of the metal-metal bonds in going from VC to CrC, although we are unable to make this a quantitative statement. (Determining the parameters of a force-constant model such as that of Weber²⁰ requires more information than ν_{opt} and the elastic constants.) We note that both the elastic constants and ν_{opt} of CrC are closer to those of NbC than to VC, and we will use this in our estimates of superconductivity.

D. Magnetism

It is often the case that an elevated $N(E_F)$ is associated with magnetic instabilities. As mentioned, we investigated whether CrC has a stable or metastable ferromagnetic state using the fixed spin-moment procedure.⁸ In this ap-

proach the total energy is calculated as a function of the total spin moment of the unit cell. Calculations for CrC were performed for several spin moments up to $1.5 \mu_B$ at the equilibrium lattice parameter. The induced moments were found to be entirely on the Cr sites, with a small opposite polarization amounting to approximately -5% of the total moment within the C spheres. As shown in Fig. 4, the total energy increases monotonically as a function of the moment and, in particular, there is no evidence of a magnetic solution. The curvature of the energy-versus-moment curve is the spin susceptibility χ . Extracting the quadratic term from a fit of the calculated energies to fourth-order even polynomial, we obtain $\chi = 4.0 \times 10^{16} \text{ emu/g}$ for CrC.

E. Superconductivity

Since we do not find a magnetic ground state for CrC, it is reasonable to ask whether CrC is a superconductor, as are some related carbides and nitrides.⁴ We investigate this issue by performing RMTA calculations of the McMillan-Hopfield parameters, using Eqs. (1)–(3). The resulting couplings are $\eta_{\text{Cr}} = 7.5 \text{ eV/\AA}^2$ and $\eta_{\text{C}} = 0.5 \text{ eV/\AA}^2$. Corresponding values for VC are 5.05 and 1.99 eV/\AA^2 , respectively.²³ The low value for η_{C} arises from the low C participation in $N(E_F)$ in CrC (see Fig. 2). As mentioned, the optic-phonon frequency and elastic constants of CrC are similar to those of NbC, implying similar force constants. Thus, as a crude approximation, we may use the known phonon spectrum of NbC to assess the prospect of superconductivity in CrC. Compared to NbC, the optic phonons in CrC are 7% lower (see above), and the acoustic phonons near Γ are approximately 15% higher (based on the density ratio and the elastic con-

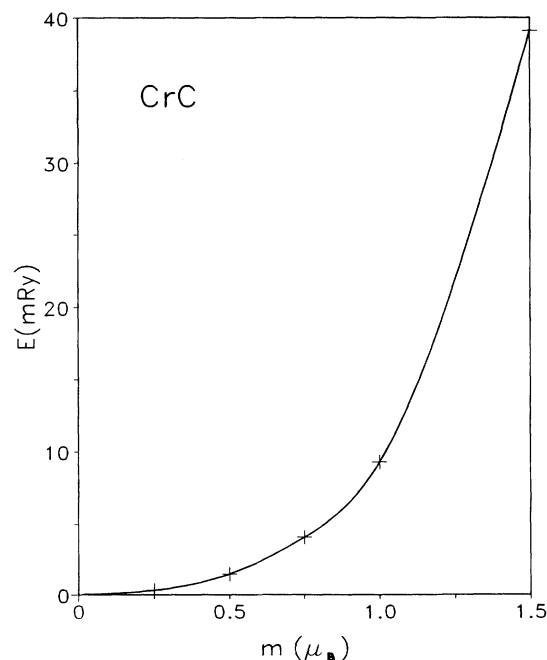


FIG. 4. Total energy as a function of the constrained spin moment m (μ_B). The solid curve is a spline interpolation of the calculated energies.

stants). Taking into account the larger Brillouin zone in CrC, we thus estimate that the average acoustic-phonon frequency is 25% higher in CrC than in NbC and that the average optic frequency is 7% lower. Using these crude estimates, and the known properties of NbC, we can obtain the electron-phonon coupling, $\lambda=0.6$, and a transition temperature in the range 5–10 K.

IV. CONCLUSIONS

Full-potential LDA-based calculations have been performed to elucidate properties of CrC. The electronic structure, magnetic stability, elastic constants, zone-center optic-phonon frequency, enthalpy of formation, and electron-phonon coupling have been calculated. The electronic structure is well described by rigid band behav-

ior based on VC. Unlike VC or NbC, the enthalpy of formation of CrC is positive (although small), implying that CrC is not a thermodynamically stable phase. However, the elastic constants and optic phonon are stable, indicating that NaCl-structure CrC is a true metastable phase. RMTA calculations of the electron phonon coupling predict that CrC is a superconductor with a transition temperature of 5–10 K.

ACKNOWLEDGMENTS

We are pleased to acknowledge informative conversations with D. A. Papaconstantopoulos. Work at NRL is supported in part by the Office of Naval Research. Some computations were performed at the Cornell National Supercomputer Facility.

*Present address: Dept. of Physics, University of California, Davis, CA 95616.

¹W. Hume-Rothery, *Philos. Mag.* **44**, 1154 (1953).

²B. X. Liu and X. Y. Cheng, *J. Phys. Condens. Matter* **4**, L265 (1992); B. X. Liu, J. Wang, X. Y. Cheng, and Z. Z. Fang, *Phys. Status Solidi (A)* **128**, K71 (1991).

³A. Neckel, P. Rastl, R. Eibler, P. Weinberger, and K. Schwarz, *J. Phys. C* **9**, 579 (1976).

⁴K. Schwarz, *CRC Crit. Rev. Solid State Mater. Sci.* **13**, 211 (1987), and references therein.

⁵V. P. Zhukov, O. I. Shikina, N. I. Medvedeva, and V. A. Gubanov, *Izv. Akad. Nauk SSSR, Neorg. Mater.* **25**, 1140 (1989) [*Inorg. Mater. (USSR)* **25**, 957 (1989)]; see also V. P. Zhukov, V. A. Gubanov, O. Jepsen, N. E. Christensen, and O. K. Andersen, *J. Phys. Chem. Solids* **49**, 841 (1988).

⁶D. L. Price and B. R. Cooper, *Phys. Rev. B* **39**, 4945 (1989).

⁷O. K. Andersen, *Phys. Rev. B* **12**, 3060 (1975); S. H. Wei and H. Krakauer, *Phys. Rev. Lett.* **55**, 1200 (1985); S. H. Wei, H. Krakauer, and M. Weinert, *Phys. Rev. B* **32**, 7792 (1985), and references therein.

⁸K. Schwarz and P. Mohn, *J. Phys. F* **14**, L129 (1984); see also A. R. Williams, V. L. Moruzzi, J. Kubler, and K. Schwarz, *Bull. Am. Phys. Soc.* **29**, 278 (1984).

⁹G. D. Gaspari and B. L. Gyorffy, *Phys. Rev. Lett.* **29**, 801 (1972); B. M. Klein and D. A. Papaconstantopoulos, *ibid.* **32**, 1193 (1974); D. A. Papaconstantopoulos and B. M. Klein, *ibid.* **35**, 110 (1975); B. M. Klein and D. A. Papaconstantopoulos, *J. Phys. F* **6**, 1135 (1976).

¹⁰D. Singh, *Phys. Rev. B* **43**, 6388 (1991).

¹¹L. Hedin and B. I. Lundqvist, *J. Phys. C* **4**, 2064 (1971); for the fixed spin-moment calculations, the spin scaling was that of U. von Barth and L. Hedin, *ibid.* **5**, 1629 (1972).

¹²The LAPW sphere radii were 2.0 a.u. for Cr and 1.70 a.u. for C atoms. The LAPW part of the basis was constructed using a cutoff wave vector K_{\max} of 4.706 a.u. Cr *s*, *p*, and *d* and C *s*

and *p* local orbitals were used to relax the linearization.

¹³A. Baldereschi, *Phys. Rev. B* **7**, 5212 (1973); D. J. Chadi and M. L. Cohen *ibid.* **8**, 5747 (1973); H. J. Monkhorst and J. D. Pack, *ibid.* **13**, 5188 (1976); **16**, 1748 (1977).

¹⁴D. D. Koelling and J. H. Wood, *J. Comp. Phys.* **67**, 253 (1986); W. E. Pickett, H. Krakauer, and P. B. Allen, *Phys. Rev. B* **38**, 2721 (1988).

¹⁵The enthalpy of formation of diamond is 0.006 eV/atom. D. D. Wagman, W. H. Evans, V. B. Parker, I. Halow, S. M. Bailey, and R. H. Schumm, NBS Technical Note 270-3 (U.S. Dept. of Commerce, Washington, D. C., 1968).

¹⁶M. J. Mehl, J. E. Osburn, D. A. Papaconstantopoulos, and B. M. Klein, *Phys. Rev. B* **41**, 10311 (1990).

¹⁷F. D. Murnaghan, *Proc. Natl. Acad. Sci. U.S.A.* **30**, 244 (1944).

¹⁸J. Chen, L. L. Boyer, H. Krakauer, and M. J. Mehl, *Phys. Rev. B* **37**, 3295 (1988).

¹⁹M. W. Chase, Jr., C. A. Davies, J. R. Downey, Jr., D. J. Fru-rip, R. A. McDonald, and A. N. Syverud, *J. Phys. Chem. Ref. Data* **14**, 1 (1985).

²⁰W. Weber, *Phys. Rev. B* **8**, 5082 (1973); in this paper elastic constants for NbC are extracted from the neutron-scattering data of Ref. 21.

²¹H. G. Smith, in *Superconductivity in d- and f-band metals*, edited by D. H. Douglass (AIP, N.Y., 1972), p. 321.

²²C-C interactions play a smaller role, since direct bonds do not form between these atoms.

²³D. Glotzel, R. W. Simpson, and H. R. Schober, *Physics of Transition Metals, 1980*, Proceedings of the "Second International Conference," edited by P. Rhodes, IOP Conf. Proc. No. 55 (Institute of Physics and Physical Society, London, 1981), p. 567; see also B. M. Klein, D. A. Papaconstantopoulos, and L. L. Boyer, in *Superconductivity in d- and f-Band Metals, Second Rochester Conference*, edited by D. H. Douglass (Plenum, New York, 1976), p. 339.